

Contents lists available at [ScienceDirect](http://www.sciencedirect.com)

# Advances in Colloid and Interface Science

journal homepage: [www.elsevier.com/locate/cis](http://www.elsevier.com/locate/cis)

## Silver nanoparticles: Green synthesis and their antimicrobial activities

Virender K. Sharma\*, Ria A. Yngard, Yekaterina Lin

Chemistry Department, Florida Institute of Technology, 150 West University Boulevard, Melbourne, Florida 32901, USA

### ARTICLE INFO

Available online 17 September 2008

#### Keywords:

Silver colloid nanoparticles  
Environmentally friendly synthesis  
Irradiation  
Silver-titanium dioxide nanoparticles  
Antibacterial

### ABSTRACT

This review presents an overview of silver nanoparticles (Ag NPs) preparation by green synthesis approaches that have advantages over conventional methods involving chemical agents associated with environmental toxicity. Green synthetic methods include mixed-valence polyoxometallates, polysaccharide, Tollens, irradiation, and biological. The mixed-valence polyoxometallates method was carried out in water, an environmentally-friendly solvent. Solutions of  $\text{AgNO}_3$  containing glucose and starch in water gave starch-protected Ag NPs, which could be integrated into medical applications. Tollens process involves the reduction of  $\text{Ag}(\text{NH}_3)_2^+$  by saccharides forming Ag NP films with particle sizes from 50–200 nm, Ag hydrosols with particles in the order of 20–50 nm, and Ag colloid particles of different shapes. The reduction of  $\text{Ag}(\text{NH}_3)_2^+$  by HTAB (*n*-hexadecyltrimethylammonium bromide) gave Ag NPs of different morphologies: cubes, triangles, wires, and aligned wires. Ag NPs synthesis by irradiation of  $\text{Ag}^+$  ions does not involve a reducing agent and is an appealing procedure. Eco-friendly bio-organisms in plant extracts contain proteins, which act as both reducing and capping agents forming stable and shape-controlled Ag NPs. The synthetic procedures of polymer-Ag and  $\text{TiO}_2$ -Ag NPs are also given. Both Ag NPs and Ag NPs modified by surfactants or polymers showed high antimicrobial activity against Gram-positive and Gram-negative bacteria. The mechanism of the Ag NP bactericidal activity is discussed in terms of Ag NP interaction with the cell membranes of bacteria. Silver-containing filters are shown to have antibacterial properties in water and air purification. Finally, human and environmental implications of Ag NPs to the ecology of aquatic environment are briefly discussed.

© 2008 Elsevier B.V. All rights reserved.

### Contents

1.	Introduction . . . . .	84
2.	Silver nanoparticles . . . . .	84
3.	Green synthesis . . . . .	84
3.1.	Polysaccharide method. . . . .	84
3.2.	Tollens method . . . . .	85
3.3.	Irradiation method . . . . .	86
3.4.	Biological method . . . . .	87
3.5.	Polyoxometallates method . . . . .	87
4.	Ag NPs and their incorporation into other materials . . . . .	87
4.1.	Silver-doped hydroxyapatite . . . . .	88
4.2.	Polymer-silver nanoparticles . . . . .	88
4.2.1.	Poly(vinyl alcohol)-silver nanoparticles . . . . .	88
4.3.	Silver nanoparticles on $\text{TiO}_2$ . . . . .	89
5.	Antimicrobial activities . . . . .	89
5.1.	Studies: mechanism . . . . .	89
5.2.	The battle against infection: Ag NPs and their incorporation into the medical field . . . . .	92
5.2.1.	Ag NPs and HIV. . . . .	93
5.3.	Antibacterial water filter. . . . .	93
5.4.	Antimicrobial air filter. . . . .	93

\* Corresponding author. Tel.: +1 321 674 7310; fax: +1 321 674 8951.  
E-mail address: [vsharma@fit.edu](mailto:vsharma@fit.edu) (V.K. Sharma).

6. Implications . . . . .	93
6.1. Human Health . . . . .	93
6.2. Environmental . . . . .	94
7. Concluding remarks . . . . .	94
Acknowledgment . . . . .	94
References . . . . .	94

## 1. Introduction

The application of nanoscale materials and structures, usually ranging from 1 to 100 nanometers (nm), is an emerging area of nanoscience and nanotechnology. Nanomaterials may provide solutions to technological and environmental challenges in the areas of solar energy conversion, catalysis, medicine, and water treatment [1,2]. This increasing demand must be accompanied by “green” synthesis methods. In the global efforts to reduce generated hazardous waste, “green” chemistry and chemical processes are progressively integrating with modern developments in science and industry. Implementation of these sustainable processes should adopt the 12 fundamental principles of green chemistry [3–7]. These principles are geared to guide in minimizing the use of unsafe products and maximizing the efficiency of chemical processes. Hence, any synthetic route or chemical process should address these principles by using environmentally benign solvents and nontoxic chemicals [3].

Nanomaterials often show unique and considerably changed physical, chemical and biological properties compared to their macro scaled counterparts [8]. Synthesis of noble metal nanoparticles for applications such as catalysis, electronics, optics, environmental, and biotechnology is an area of constant interest [9–15]. Gold, silver, and copper have been used mostly for the synthesis of stable dispersions of nanoparticles, which are useful in areas such as photography, catalysis, biological labeling, photonics, optoelectronics and surface-enhanced Raman scattering (SERS) detection [16,17]. Additionally, metal nanoparticles have a surface plasmon resonance absorption in the UV–Visible region. The surface plasmon band arises from the coherent existence of free electrons in the conduction band due to the small particle size [18,19]. The band shift is dependent on the particle size, chemical surrounding, adsorbed species on the surface, and dielectric constant [20]. A unique characteristic of these synthesized metal particles is that a change in the absorbance or wavelength gives a measure of the particle size, shape, and interparticle properties [20,21]. Moreover, functionalized, biocompatible and inert nanomaterials have potential applications in cancer diagnosis and therapy [22–26]. The target delivery of anticancer drugs has been done using nanomaterials [22]. With the use of fluorescent and magnetic nanocrystals, the detection and monitoring of tumor biomarkers have been demonstrated [24,25].

Generally, metal nanoparticles can be prepared and stabilized by physical and chemical methods; the chemical approach, such as chemical reduction, electrochemical techniques, and photochemical reduction is most widely used [27,28]. Studies have shown that the size, morphology, stability and properties (chemical and physical) of the metal nanoparticles are strongly influenced by the experimental conditions, the kinetics of interaction of metal ions with reducing agents, and adsorption processes of stabilizing agent with metal nanoparticles [21,22]. Hence, the design of a synthesis method in which the size, morphology, stability and properties are controlled has become a major field of interest [29].

## 2. Silver nanoparticles

Silver is widely known as a catalyst for the oxidation of methanol to formaldehyde and ethylene to ethylene oxide [30]. In the United States, more than  $4 \times 10^6$  tons of silver were consumed in 2000.

Colloidal silver is of particular interest because of distinctive properties, such as good conductivity, chemical stability, catalytic and antibacterial activity [31]. For example, silver colloids are useful substrates for surface enhanced spectroscopy (SERS), since it partly requires an electrically conducting surface [19,32,33]. Also, the exposure of silver ions to light reduces them into 3–5 atoms clusters of silver, which catalyzes a gain of  $\sim 10^8$  atoms in latent image to be visible [34].

Chemical reduction is the most frequently applied method for the preparation of silver nanoparticles (Ag NPs) as stable, colloidal dispersions in water or organic solvents [35,36]. Commonly used reductants are borohydride, citrate, ascorbate, and elemental hydrogen [37–45]. The reduction of silver ions ( $\text{Ag}^+$ ) in aqueous solution generally yields colloidal silver with particle diameters of several nanometers [36]. Initially, the reduction of various complexes with  $\text{Ag}^+$  ions leads to the formation of silver atoms ( $\text{Ag}^0$ ), which is followed by agglomeration into oligomeric clusters [46]. These clusters eventually lead to the formation of colloidal Ag particles [46]. When the colloidal particles are much smaller than the wavelength of visible light, the solutions have a yellow color with an intense band in the 380–400 nm range and other less intense or smaller bands at longer wavelength in the absorption spectrum [19,32,33]. This band is attributed to collective excitation of the electron gas in the particles, with a periodic change in electron density at the surface (surface plasmon absorption) [47–49].

Previous studies showed that use of a strong reductant such as borohydride, resulted in small particles that were somewhat monodisperse, but the generation of larger particles was difficult to control [50,51]. Use of a weaker reductant such as citrate, resulted in a slower reduction rate, but the size distribution was far from narrow [37,38,52]. Controlled synthesis of Ag NPs is based on a two-step reduction process [51]. In this technique a strong reducing agent is used to produce small Ag particles, which are enlarged in a secondary step by further reduction with a weaker reducing agent [37]. Different studies reported the enlargement of particles in the secondary step from about 20–45 nm to 120–170 nm [53–55]. Moreover, the initial sol was not reproducible and specialized equipment was needed [39]. The syntheses of nanoparticles by chemical reduction methods are therefore often performed in the presence of stabilizers in order to prevent unwanted agglomeration of the colloids.

The green synthesis of Ag NPs involves three main steps, which must be evaluated based on green chemistry perspectives, including (1) selection of solvent medium, (2) selection of environmentally benign reducing agent, and (3) selection of nontoxic substances for the Ag NPs stability [7]. Based on this approach, we have reviewed the green-chemistry type Ag NP synthesis processes. The synthesis of polymer-Ag NPs and Ag NPS on  $\text{TiO}_2$  are also summarized because of their industrial and environmental importance. Finally, antimicrobial activities of Ag NPs with some examples of mechanism are presented. Implications of Ag NPs to human health and environment are briefly discussed.

## 3. Green synthesis

### 3.1. Polysaccharide method

In this method, Ag NPs are prepared using water as an environmentally benign solvent and polysaccharides as a capping

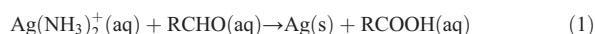
agent, or in some cases polysaccharides serve as both a reducing and a capping agent. For instance, synthesis of starch-Ag NPs was carried out with starch as a capping agent and  $\beta$ -D-glucose as a reducing agent in a gently heated system [7]. The starch in the solution mixture avoids use of relatively toxic organic solvents [56]. Additionally, the binding interactions between starch and Ag NPs are weak and can be reversible at higher temperatures, allowing separation of the synthesized particles.

In a case of dual polysaccharide function, Ag NPs were synthesized by the reduction of  $\text{Ag}^+$  inside of nanoscopic starch templates, Fig. 1. The extensive network of hydrogen bonds in the templates provides surface passivation or protection against nanoparticle aggregation [7,57]. Also, Ag NPs were synthesized by using negatively charged heparin as a reducing/stabilizing agent by heating a solution of  $\text{AgNO}_3$  and heparin to  $70^\circ\text{C}$  for  $\sim 8$  h [58]. TEM images of these Ag NPs revealed an increase in particle size with increased concentrations of both,  $\text{AgNO}_3$  and heparin [58]. Furthermore, changes in heparin concentration varied Ag NP size and morphology suggesting that heparin must behave as a nucleation controller and stabilizer [58]. The Ag NPs were highly stable and showed no signs of aggregation after two months [58].

In another study, stable Ag NPs (10–34 nm) were synthesized by autoclaving a solution of  $\text{AgNO}_3$  and starch (capping/reducing agent) at 15 psi and  $121^\circ\text{C}$  for 5 min [59]. The Ag NPs were stable in solution for three months at  $\sim 25^\circ\text{C}$ . Smaller Ag NPs ( $\leq 10$  nm) were produced by mixing two solutions of  $\text{AgNO}_3$  containing starch, a capping agent, and NaOH solutions containing glucose, a reducing agent, in a spinning disk reactor with a reaction time of less than 10 min [60]. Importantly, starch-protected nanoparticles can be easily integrated into systems for biological and pharmaceutical applications.

### 3.2. Tollens method

The Tollens synthesis method gives Ag NPs with a controlled size in a one-step process [61–64]. The basic Tollens reaction involves the reduction of  $\text{Ag}(\text{NH}_3)_2^+(\text{aq})$ , a Tollens reagent, by an aldehyde, Eq. (1).



In the modified Tollens procedure,  $\text{Ag}^+$  ions are reduced by saccharides in the presence of ammonia, yielding Ag NP films with particle sizes from 50–200 nm, Ag hydrosols with particles in the order of 20–50 nm, and Ag NPs of different shapes [62,63].  $\text{Ag}(\text{NH}_3)_2^+$  is a stable complex ion resulting from ammonia's strong affinity for  $\text{Ag}^+$ , therefore the ammonia concentration and nature of the reductant must play a major role in controlling the Ag NP size [63].

To better understand the synthesis process lets consider this example. A research study on the saccharide reduction of  $\text{Ag}^+$  ions by the modified Tollens process revealed that the smallest particles were formed at the lowest ammonia concentration [63]. Specifically,

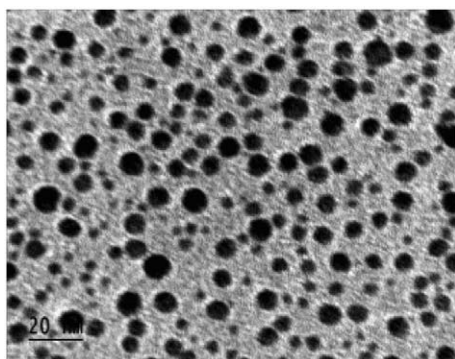


Fig. 1. Typical TEM image of starch silver nanoparticles. The scale bar corresponds to 20 nm (reproduced from [7] with permission from the American Chemical Society).

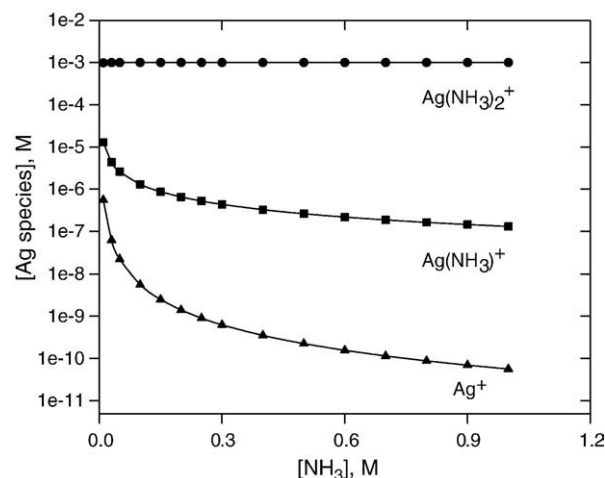


Fig. 2. Concentration of free  $\text{Ag}^+$  ions and silver–ammonia complexes versus the ammonia concentration. The total [silver]=0.001 M.

glucose and the lowest ammonia concentration, 0.005 M, resulted in the smallest average particle size of 57 nm with an intense maximum of the surface plasmon absorbance at 420 nm. Furthermore, a simultaneous increase in particle size and polydispersity was detected with an increase in  $[\text{NH}_3]$  from 0.005 M to 0.2 M [63].

To gain further insight on the effect of ammonia, it is important to know the chemical speciation of  $\text{Ag}(\text{I})$  in the studied system. Both, Ag

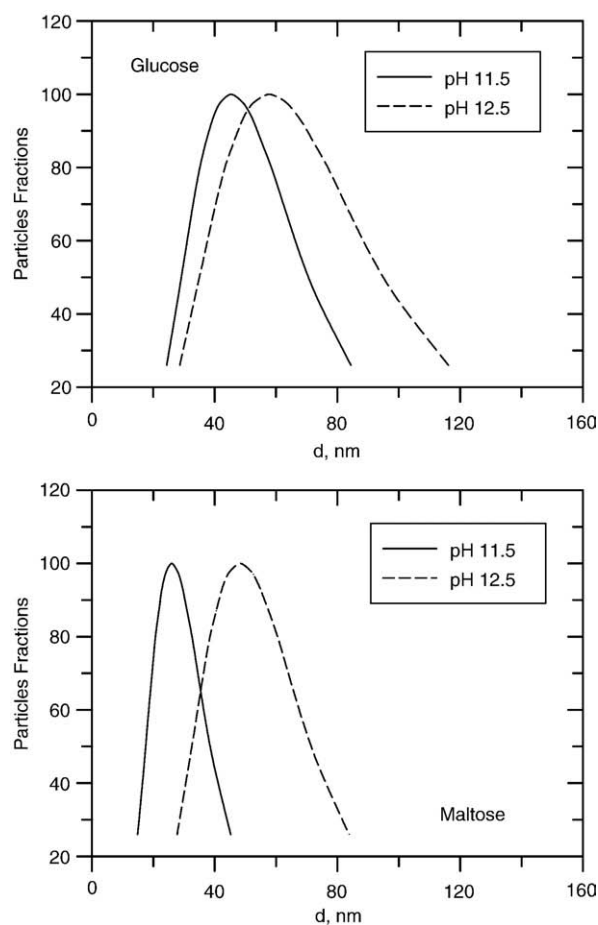


Fig. 3. Log-normal size distribution of silver nanoparticles at different pH for glucose and maltose in 0.005 M ammonia concentration (reproduced from [66] with permission from the American Chemical Society).

$(\text{NH}_3)^+$  and  $\text{Ag}(\text{NH}_3)_2^+$  are produced in the reaction solution as shown in Eqs. (2) and (3), where the formation constants are  $\log \beta_1 = 3.367$  and  $\log \beta_2 = 7.251$ , respectively [65].



The concentrations of the possible Ag species using formation constants expressed in Eqs. (2) and (3) as a function of  $[\text{NH}_3]$  are displayed in Fig. 2. A decrease in  $[\text{Ag}^+]$  in the presence of  $\text{NH}_3$  results in a decrease in the reduction rate to  $\text{Ag}(\text{s})$ , Eq. (1), and thus is reflected in the particle size. Initially this would lead to a decrease in the formation of stable Ag nuclei. In the latter stage of particle growth, the limited presence of nuclei would lead to larger particles.

Likewise, Ag NPs of controllable sizes were synthesized by reduction of  $[\text{Ag}(\text{NH}_3)_2]^+$  with two monosaccharides (glucose and galactose) and two disaccharides (maltose and lactose) [66]. The synthesis was carried out at various ammonia concentrations (0.005–0.20 M) and pH conditions (11.5–13.0) resulting in average particle sizes of 25–450 nm. As anticipated, the average particle size increased with increasing  $[\text{NH}_3]$ . A maximum particle size was reached at the concentration of 0.035 M for disaccharides and 0.20 M for monosaccharides. The difference in structure of monosaccharides and disaccharides influences the particle size with disaccharides giving on average smaller particles than monosaccharides at pH 11.5 (e.g. Fig. 3). Furthermore, particles obtained at pH 11.5 were smaller than those at pH 12.5. Polydispersity also decreased by lowering the pH (Fig. 3). Maltose gave Ag NPs with the most narrow size distribution and the smallest average size of 25 nm. To extend shelf life, Ag NPs were

stabilized by two surfactants, sodium dodecyl sulfate-SDS and polyoxyethylenesorbitane monooleate-Tween 80, and a polymer, polyvinylpyrrolidone-PVP 360 [67,68].

A modified Ag mirror reaction (Tollens reaction) is an example of a synthesis route yielding Ag NPs of different shapes. Ag NPs of various morphologies with <10 nm diameters were synthesized in water by adjusting the concentrations of *n*-hexadecyltrimethylammonium bromide (HTAB) and the Tollens reagent,  $\text{Ag}(\text{NH}_3)_2^+$ , at 120 °C [69,70]. TEM images of Ag NPs obtained by this method are shown in Fig. 4.

### 3.3. Irradiation method

Ag NPs can be successfully synthesized by using a variety of irradiation methods. For example, laser irradiation of an aqueous solution of Ag salt and surfactant can fabricate Ag NPs with a well-defined shape and size distribution [71]. No reducing agent is required in this method. Additionally, laser was applied in a photo-sensitization technique for the synthesis of Ag NPs using benzophenone [72]. Here, low laser powers at short irradiation times gave Ag NPs of ~20 nm, while an increased irradiation power gave nanoparticles of ~5 nm. The formation of Ag NPs by this photo-sensitization technique was also achieved using a mercury lamp [72]. In the visible light irradiation studies, photo-sensitized growth of Ag NPs using thiophene as a sensitizing dye [73] and Ag NP production by illumination of  $\text{Ag}(\text{NH}_3)^+$  in ethanol has been carried out [74].

Synthesis procedures using microwave irradiation has also been employed. Microwave radiation of a carboxymethyl cellulose sodium and silver nitrates solution produced uniform Ag NPs that were stable for two months at room temperature [75]. The microwave irradiation

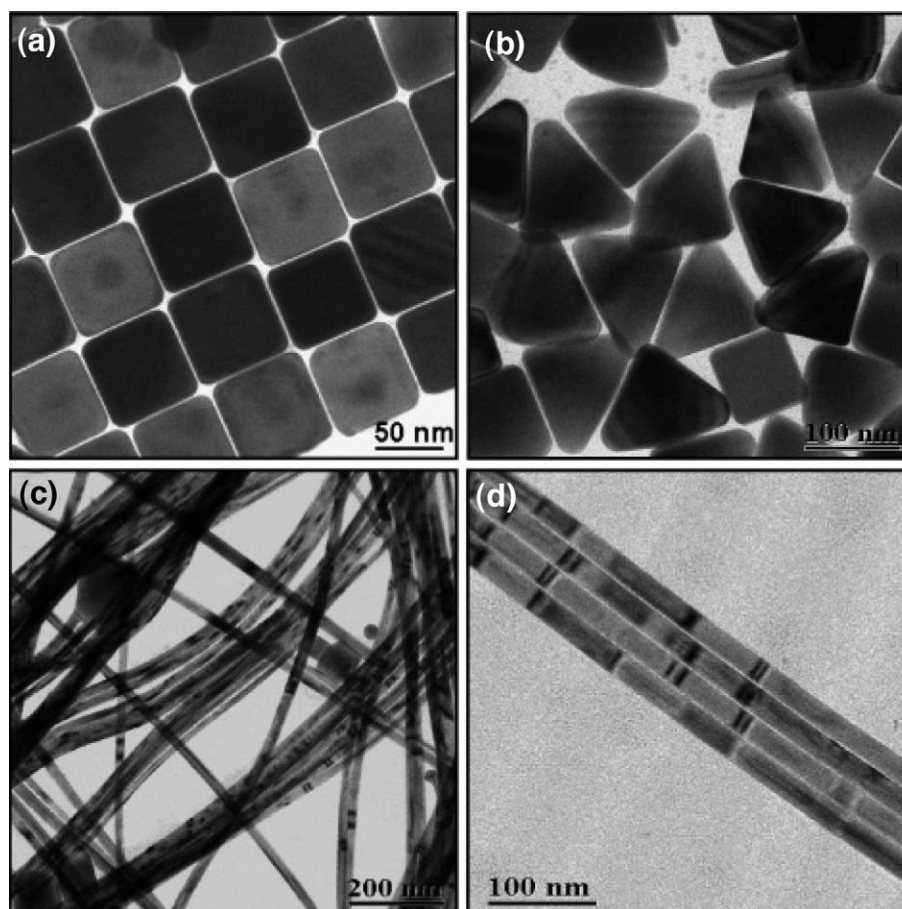


Fig. 4. TEM images of silver nanoparticles: (a) cubes; (b) triangles; (c) wires; (d) an alignment of wires. (reproduced from [70] with permission from the American Chemical Society).

of a  $\text{AgNO}_3$ -ethylene-glycol- $\text{H}_2[\text{PtCl}_6]$ -poly(vinylpyrrolidone) solution gave Ag NPs of different shapes within 3 min. [76]. Recently, the use of microwave radiation to synthesize nearly monodisperse Ag NPs using basic amino acids as reducing agents and soluble starch as a protecting agent has been shown [77].

Ionizing radiation can reduce  $\text{Ag}^+$  ions in Ag NPs synthesis [78–83]. In one study, Ag NPs of > 10 nm were produced in supercritical ethane at 80 °C and 80–120 bar with methanol as a solvent [78]. The solvated electrons reduced the  $\text{Ag}^+$  ions and a characteristic plasmon absorption was detected within 1–10 s after the ionization pulse.

Furthermore, radiolysis has been applied in the Ag NP production. The radiolysis of  $\text{Ag}^+$  ions in ethylene glycol was studied [82]. Here, the formation of  $\text{Ag}^0$  was observed at 350 nm ( $k(\text{Ag}^+ + e_{\text{solv}}^-) = 2.8 \times 10^9 \text{ M}^{-1} \text{ s}^{-1}$ ) and the surface plasmon band appeared slowly at 400 nm with a coalescence cascade  $k = 2 \times 10^6 \text{ M}^{-1} \text{ s}^{-1}$  [82]. Furthermore, Ag NPs supported on silica aerogel were synthesized using gamma radiolysis [83]. The Ag clusters were stable in the 2–9 pH range and started agglomeration at pH > 9 [83]. In another work, oligochitosan as a stabilizer was used in preparation of Ag NPs by gamma radiation synthesizing 5–15 nm stable Ag NPs in a 1.8–9.0 pH range [79]. Gamma radiation in acetic water solution containing  $\text{AgNO}_3$  and chitosan gave particles with an average diameter of 4–5 nm [80]. Ag NPs of different size (60–200 nm) have also been synthesized by irradiating a solution, prepared by mixing  $\text{AgNO}_3$  and poly-vinyl-alcohol, with 6 MeV electrons [84]. The variation of electron fluence from  $2 \times 10^{13}$ – $3 \times 10^{15} \text{ e cm}^{-2}$  produced Ag NPs of narrow size distribution (60–10 nm) [84].

The pulse radiolysis technique has been applied to study the reactions of inorganic and organic species in Ag NP synthesis [85–87]. This technique was successfully applied to understand the factors controlling the shape and size of Ag NPs produced by a common reduction method using citrate ions [88]. Interestingly, the citrate ion functioned as a reductant, a complexant, and a stabilizer. Recently, a pulse radiolysis study was performed to demonstrate the role of phenol derivatives in the formation of Ag NPs by the reduction of  $\text{Ag}^+$  ions with dihydroxybenzene [89].

In a morphology conversion study, suspensions of Ag nanospheres were converted to triangular Ag nanocrystals, so called nanoprisms, in high yield using photoinduced electron transfer [90]. This photo-induced method was extended to demonstrate synthesis of relatively monodisperse nanoprisms with desired edge lengths of 30–120 nm [91]. With the use of dual-beam illumination, the nanoparticle growth process could be controlled.

### 3.4. Biological method

Extracts from bio-organisms may act both as reducing and capping agents in Ag NPs synthesis. The reduction of  $\text{Ag}^+$  ions by combinations of biomolecules found in these extracts such as enzymes/proteins, amino acids, polysaccharides, and vitamins [92,93] is environmentally benign, yet chemically complex. An extensive volume of literature reports successful Ag NP synthesis using bioorganic compounds.

For example, the extract of unicellular green algae *Chlorella vulgaris* was used to synthesize single-crystalline Ag nanoplates at room temperature [94]. Proteins in the extract provide dual function of  $\text{Ag}^+$  reduction and shape-control in the nanosilver synthesis. The carboxyl groups in aspartic and/or glutamine residues and the hydroxyl groups in tyrosine residues of the proteins were suggested to be responsible for the  $\text{Ag}^+$  ion reduction [94]. Carrying out the reduction process by a simple bifunctional tripeptide Asp-Asp-Tyr-OME further identified the involvement of these residues. This synthesis process gave small Ag nanoplates with low polydispersity in good yield (>55%) [94].

Plant extracts from live alfalfa, the broths of lemongrass, geranium leaves and others have served as green reactants in Ag NP synthesis [95–97]. The reaction of aqueous  $\text{AgNO}_3$  with an aqueous extract of leaves of a common ornamental geranium plant, *Pelargonium grave-*

*olens*, gave Ag NPs after 24 h [96]. The reaction time was reduced to 2 h by heating the reaction mixture just below the boiling point [98]. Secreted proteins in spent mushroom substrate reduced  $\text{Ag}^+$  to give uniformly distributed Ag-protein (core-shell) NPs with an average size of 30.5 nm [99]. A vegetable, *Capsicum annum* L., was used to also synthesize Ag NPs [100].

Studying the synthesis of Ag NPs with isolated/purified bioorganics may give better insight into the system mechanism. Glutathione ( $\gamma$ -Glu-Cys-Gly-) as a reducing/capping agent can produce water-soluble and size tunable Ag NPs that easily bind to model protein (bovine serum albumin) – attractive for medical applications [101]. Tryptophan residues of synthetic oligopeptides at the C-terminus were identified as reducing agents giving Ag NPs [102]. Furthermore, Ag NPs were successfully synthesized by Vitamin E in the Langmuir-Blodgett technique, by biosurfactants, such as sophorolipids, [103–105] and by L-Valine-based oligopeptides with chemical structures, Z-(L-Val)<sub>3</sub>-OME and Z-(L-Val)<sub>2</sub>-L-Cys(S-Bzl)-OME [106]. The sulfur content in the Z-(L-Val)<sub>2</sub>-L-Cys(S-Bzl)-OME controls the shape and size of Ag NPs, which suggests the interaction between the  $\text{Ag}^+$  ion and the thioether moiety of the peptide [106]. Oleic acid has also been used in environmentally-friendly synthesis of organic-soluble Ag NPs [107].

Several microorganisms have been utilized to grow Ag NPs intracellularly or extracellularly [108–114]. For instance, Ag containing nanocrystals of different compositions were synthesized by *Pseudomonas stutzeri* AG259 bacterium [108]. In *Fusarium oxysporum* fungus, the reduction of  $\text{Ag}^+$  ions was attributed to an enzymatic process involving NADH-dependent reductase [113]. The white rot fungus, *Phanerochaete chrysosporium*, also reduced  $\text{Ag}^+$  ion to form Ag NPs; a protein was suggested to cause the reduction [114]. Possible involvement of proteins in synthesizing Ag NPs was observed in filamentous cyanobacterium, *Plectonema boryanum* UTEX 485 [115]. Moreover,  $\text{Ag}^+$  reduction by culture supernatants of *Klebsiella pneumoniae*, *Escherichia coli* (*E. coli*), and *Enterobacter cloacae* (*Enterobacteriaceae*) produced rapid formations of Ag NPs [116].

### 3.5. Polyoxometalates method

Polyoxometalates, POMs, have the potential of synthesizing Ag NPs because they are soluble in water and have the capability of undergoing stepwise, multielectron redox reactions without disturbing their structure [117–119]. For example, Ag NPs were synthesized by illuminating a deaerated solution of POM/S/ $\text{Ag}^+$  (POM:  $[\text{PW}_{12}\text{O}_{40}]^{3-}$ ,  $[\text{SiW}_{12}\text{O}_{40}]^{4-}$ ; S: prpan-2-ol or 2,4-dichlorophenol) [119]. In this method POMs serve both as a photocatalyst, a reducing agent, and as a stabilizer [119]. In another study, one-step synthesis and stabilization of Ag nanostructures with Mo<sup>V</sup>-Mo<sup>VI</sup> mixed-valence POMs in water at room temperature has been demonstrated [120]. This method did not use a catalyst or a selective etching agent.

Ag NPs of different shape and size can be obtained using different POMs in which the POMs serve as a reductant and a stabilizer. For instance, a salt,  $\text{Ag}_2\text{SO}_4$ , and POMs,  $(\text{NH}_4)_{10}[\text{Mo}^{\text{V}}_4(\text{Mo}^{\text{VI}})_2\text{O}_{14}(\text{O}_3\text{PCH}_2\text{PO}_3)_2(\text{HO}_3\text{PCH}_2\text{PO}_3)_2]$ -15  $\text{H}_2\text{O}$  and  $\text{H}_7[\beta\text{-P}(\text{Mo}^{\text{VI}})_4(\text{Mo}^{\text{VI}})_8\text{O}_{40}]$ , were reacted. After several minutes of mixing a characteristic SPR band at 400 nm for Ag NPs appeared and the location of the peak was not significantly affected by the initial concentration of  $\text{Ag}_2\text{SO}_4$  (Fig. 5a) [120]. The Ag NPs obtained were spherical and quasi-monodispersed with a diameter of ~38 nm (Fig. 5b), the particle size distribution was quantitatively displayed in a histogram (Fig. 5c). The single Ag NP in Fig. 5d has a Ag-POM core-shell structure with a ~2 nm thick POM layer.

## 4. Ag NPs and their incorporation into other materials

The unique properties of Ag NPs have been extended into a broader range of applications. Incorporation of Ag NPs with other materials is an attractive method of increasing compatibility for specific applications.

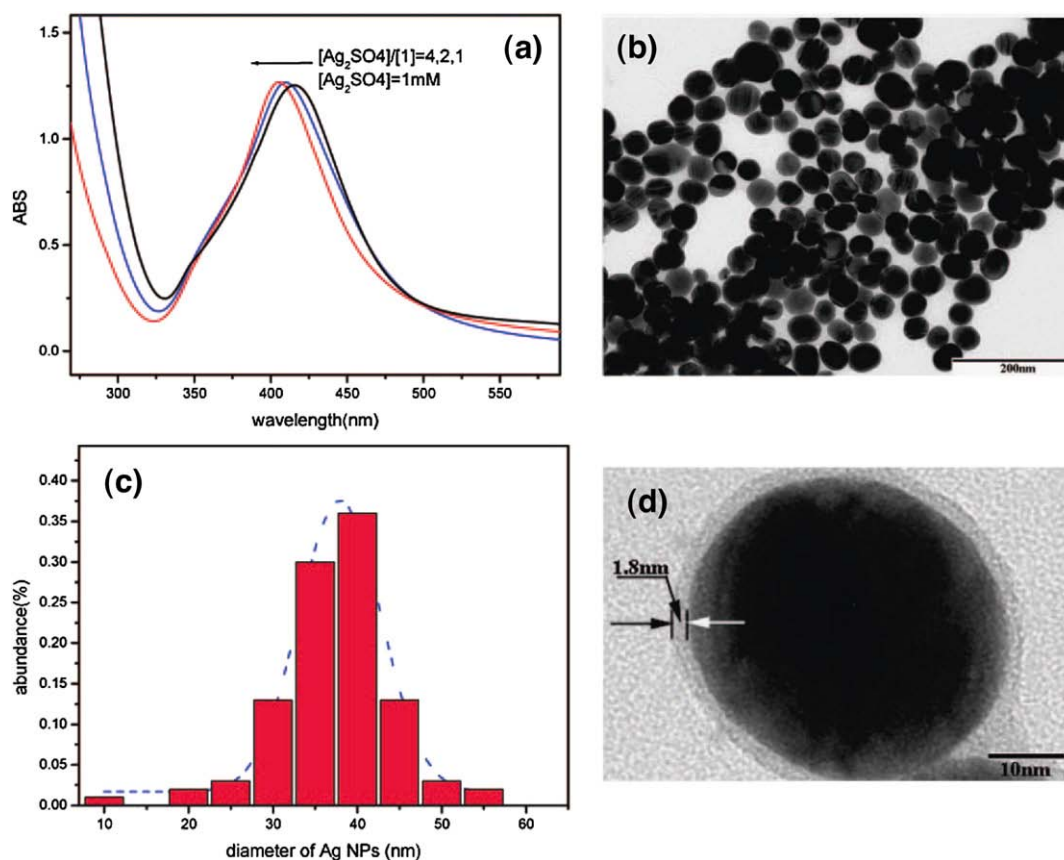


**Fig. 5.** (a) SPR spectra of Ag nanoparticles obtained from different molar ratios, (b) a representative TEM image of Ag nanoparticles obtained from the mixture with  $\gamma$  4, (c) size histogram of Ag nanoparticles of about 200 NPs counted from TEM image showing the distribution of Ag NPs, and (d) a magnified Ag nanoparticle. (reproduced from [70] with permission from the American Chemical Society).

#### 4.1. Silver-doped hydroxyapatite

There is interest in inorganic-inorganic hybrid nanocomposites materials because of their industrial and medical applications [121–124]. Recently, one-step synthesis of anisotropic Ag nanocrystals was achieved by reducing aqueous  $Ag^+$  ion by the electron transfer from the surface of hydroxyapatite (HA) [125]. The hydroxyl group in this process acted both as a reducing and a binding agent to give highly oriented flat rod and needle-like Ag NPs [125]. A microwave process was also applied to synthesize nanosize Ag-substituted HA with a length of 60–70 nm and width of 15–20 nm [126].

#### 4.2. Polymer-silver nanoparticles

Nanocomposite materials consisting of metallic nanoparticles incorporated in or with polymers have attracted much attention because of their distinct optical, electrical and catalytic properties, which have potential applications in the fields of catalysis, bioengineering, photonics, and electronics [47,127–130]. Polymers are considered a good host material for metal nanoparticles as well as other stabilizing agents such as citrates, organic solvents (THF or THF/MeOH), long chain alcohols, surfactants, and organometallics [9,131,132]. The organic solvents are though not as environmental benign.

Different chemical and physical methods exist to prepare metal-polymer composites [46,133,134–142]. A successful preparation of nanoparticles is determined by the ability to produce particles with uniform distributions and long stability, given their tendency to rapidly agglomerate in aqueous solution [130,133]. The main fabrication approach is to disperse previously prepared particles in the polymer matrix [141,142]. This method is often referred to as the

evaporation method since the polymer solvent is evaporated from the reaction mixture after NP dispersion. However, this often leads to inhomogeneous distribution of the particles in the polymer. One solution is the *in situ* synthesis of metal particles in the polymer matrix, which involves the dissolution and reduction of metal salts or complexes into the matrix [138,143]. Or, another approach is a system in which simultaneous polymerization and metal reduction occur.

For example, the *in situ* reduction of  $Ag^+$  ions in poly(*N*-vinyl-2-pyrrolidone) (PVP) by microwave irradiation produced particles with narrow size distribution [144] and Ag NPs incorporated in acacia, a natural polymer, had been made under mild condition [145]. Or, a conventional heating method to polymerize acrylonitrile simultaneously reduces  $Ag^+$  ions resulting in homogeneous dispersal and narrow size distributions of the Ag NPs in the silver-polyacrylonitrile (Ag-PAN) composite powders [138]. Further, size-controlled synthesis of a Ag nanocomplex was recently achieved in the reduction of  $AgNO_3$  by a UV-irradiated arginine-tungstonsilicate acid solution [146]. Other various metal-polymer nanocomposites have been prepared by these reduction methods, such as poly(vinyl alcohol)-Ag, Ag-polyacrylamide, Ag-acrylonitrile (Ag-PAN),  $Ag_2Se$ -polyvinyl alcohol, Ag-polyimide, Au-polyaniline, and Cu-poly(acrylic acid) [143,147]. Due to its growing importance in a multitude of industries, let's explore poly(vinyl alcohol)-Ag synthesis and applications in more detail.

##### 4.2.1. Poly(vinyl alcohol)-silver nanoparticles

Poly(vinyl alcohol) (PVA) is a biologically friendly polymer since it is water soluble and has extremely low cytotoxicity [148]. This allows a wide range of potential biomedical applications. It is frequently used as a stabilizer due to its optical clarity, which enables investigation of the nanoparticle formation [149,150]. PVA is classified into grades of partially (85–89%) and fully (97–99.5%) hydrolyzed polymers (Fig. 6).

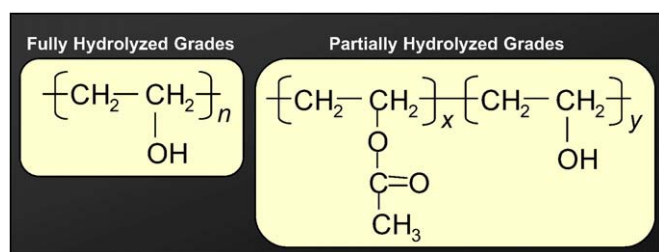


Fig. 6. Structure of fully hydrolyzed and partially hydrolyzed PVA.

PVA is widely used in various industries such as textile, paper, food packaging, pharmacy, and cosmetics [151]. Introduction of nanosized Ag into PVA provides antibacterial activity, which is highly desired in textiles used in medicine, clothing and household products [151]. However, this can significantly affect the properties of the polymer due to the high surface to bulk ratio of Ag NPs. [150–153].

Different methods including solvent evaporation, electron radiation, UV light, thermal annealing, *in situ* chemical reduction, and sonochemical have been proposed to synthesize PVA-Ag NPs [154–166]. And a variety of morphologies were obtained under different preparation conditions. In the solvent evaporation methods, the synthesis of PVA-Ag NPs was achieved by first reducing Ag salt with  $\text{NaBH}_4$ , followed by the mechanical dispersion of the Ag colloids into the dissolved polymer, and then the solvent was evaporated resulting in final structure [154]. The initial average particle size of 5 nm with narrow size distribution increased to 20 nm with a broad surface plasmon absorption band after the dispersion [154]. This particle agglomeration during the incorporation into the PVA matrix resulted in significant changes in the thermal and mechanical properties of the polymer [154]. The electron and UV radiation preparation methods involve irradiation of a  $\text{Ag}^+$  doped polymer film which gives PVA-Ag composites [159–161]. In thermal methods, the annealing time and temperature vary the morphologies of the PVA-Ag NPs [165,166]. For instance, hydrogels of PVA-PVP (poly(*N*-vinyl pyrrolidone) containing Ag NPs were prepared by repeated freezing–thawing treatment [167]. The hydrogels have unique properties because of their three-dimensional hydrophilic polymer networks, which provide a wide range of pharmaceuticals and medical applications [168]. Using *in situ* chemical reduction, our laboratory had recently synthesized Ag NPs of controlled size by the modified Tollens process with PVA as a stabilizer and reductant [169]. Briefly, one drop of 0.02 M NaOH was added to 2 ml of 1 mM  $\text{AgNO}_3$ , followed by 3 drops of 0.2 M  $\text{NH}_4\text{OH}$  and 0.25 ml 1% aqueous PVA solution. Gentle heating for 2 min resulted in a yellow colored mixture. The visible spectrum showed a maximum at 422 nm, indicating the formation of PVA-Ag NPs (Fig. 7).

#### 4.3. Silver nanoparticles on $\text{TiO}_2$

Silver/ $\text{TiO}_2$  surfaces have advantageous properties such as visible light photocatalysis, biological compatibility, and antimicrobial activity [170–176]. Aqueous reduction, photochemical, liquid phase deposition, and sol–gel methods can be applied to synthesize Ag NPs on  $\text{TiO}_2$  surfaces [177–182]. Ag NPs with a narrow size distribution were synthesized by simple aqueous reduction from silver ions in different molar ratios of  $\text{TiO}_2$  suspensions and a reducing agent,  $\text{NaBH}_4$  [178]. One of the photochemical reduction methods involves loading Ag NPs with ~3–5 nm diameters onto the surface of  $\text{TiO}_2$  nanotubes first using the liquid deposition approach followed by UV [179] or by femtosecond laser irradiation [181].

In another photoreduction example, Ag– $\text{TiO}_2$  nanocomposites and PVA-capped colloidal Ag– $\text{TiO}_2$  nanocomposites have been prepared to investigate their antibacterial activity in *E. coli* and *Bacillus subtilis* [182]. Photoreduction of  $\text{AgNO}_3$  at 365 nm wavelength using bare  $\text{TiO}_2$  and PVA-capped colloidal  $\text{TiO}_2$  nanoparticles/nanotubes was carried

out. The TEM images of these nanocomposites are given in Fig. 8. The reactants,  $\text{TiO}_2$  particles and  $\text{TiO}_2$  nanotubes, were well dispersed in their reaction mixtures having a ~25 nm particle size and a ~20 nm nanotube diameter with a length of ~250 nm, respectively (a and b). In the images of the resulting 5 wt.% Ag– $\text{TiO}_2$  nanocomposites, the Ag on the  $\text{TiO}_2$  nanoparticles was difficult to visualize (c) yet Ag on the  $\text{TiO}_2$  nanotubes was clearly evident (d). Next, *in-situ* PVA-capped  $\text{TiO}_2$  nanoparticles, ~20 nm particle size, and PVA-capped  $\text{TiO}_2$  nanotubes were prepared (e and f). Photoreduction on these nanocomposites products caused Ag aggregation into fairly large colloids. The Ag in PVA-capped Ag– $\text{TiO}_2$  particles formed Ag clusters of sizes ~15 nm (g), while Ag on the PVA-capped Ag– $\text{TiO}_2$  nanotubes gave larger, ~40 nm, Ag particle sizes (h). This work reports that low concentration of colloidal Ag– $\text{TiO}_2$  nanoparticles and nanotubes were effective in destroying *E. coli* and *B. subtilis* [182].

## 5. Antimicrobial activities

Silver is known for its antimicrobial properties and has been used for years in the medical field for antimicrobial applications and even has shown to prevent HIV binding to host cells [178,183–186]. Additionally, silver has been used in water and air filtration to eliminate microorganisms [187–189].

### 5.1. Studies: mechanism

The mechanism of the bactericidal effect of silver and Ag NPs remains to be understood. Several studies propose that Ag NPs may attach to the surface of the cell membrane disturbing permeability and respiration functions of the cell [67]. Smaller Ag NPs having the large surface area available for interaction would give more bactericidal effect than the larger Ag NPs [67]. It is also possible that Ag NPs not only interact with the surface of membrane, but can also penetrate inside the bacteria [190].

In one study, the Ag NPs obtained in the reduction of the  $\text{Ag}(\text{NH}_3)_2^+$  complex cation by four saccharides with narrow size distribution were tested as antimicrobial agents (Table 1) [66]. Table 1 shows that Ag NPs synthesized using disaccharides, maltose and lactose, have a higher antibacterial activity than those synthesized using monosaccharides, glucose and galactose. The sizes of the colloidal Ag particles were smaller for disaccharide than monosaccharide and thus may be responsible for the observed antibacterial activity. The 25 nm-sized Ag NPs synthesized via reduction by maltose (see Table 1) showed the highest activity and were comparable to the effects of ionic silver in certain bacteria strains. Galactose had the largest Ag NPs particles, 50 nm, and gave the lowest antimicrobial effect [66].

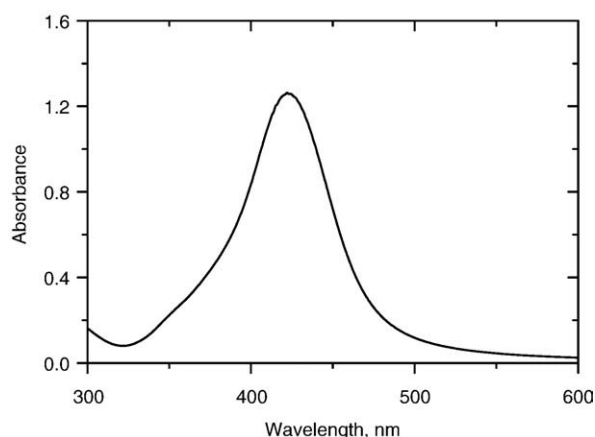
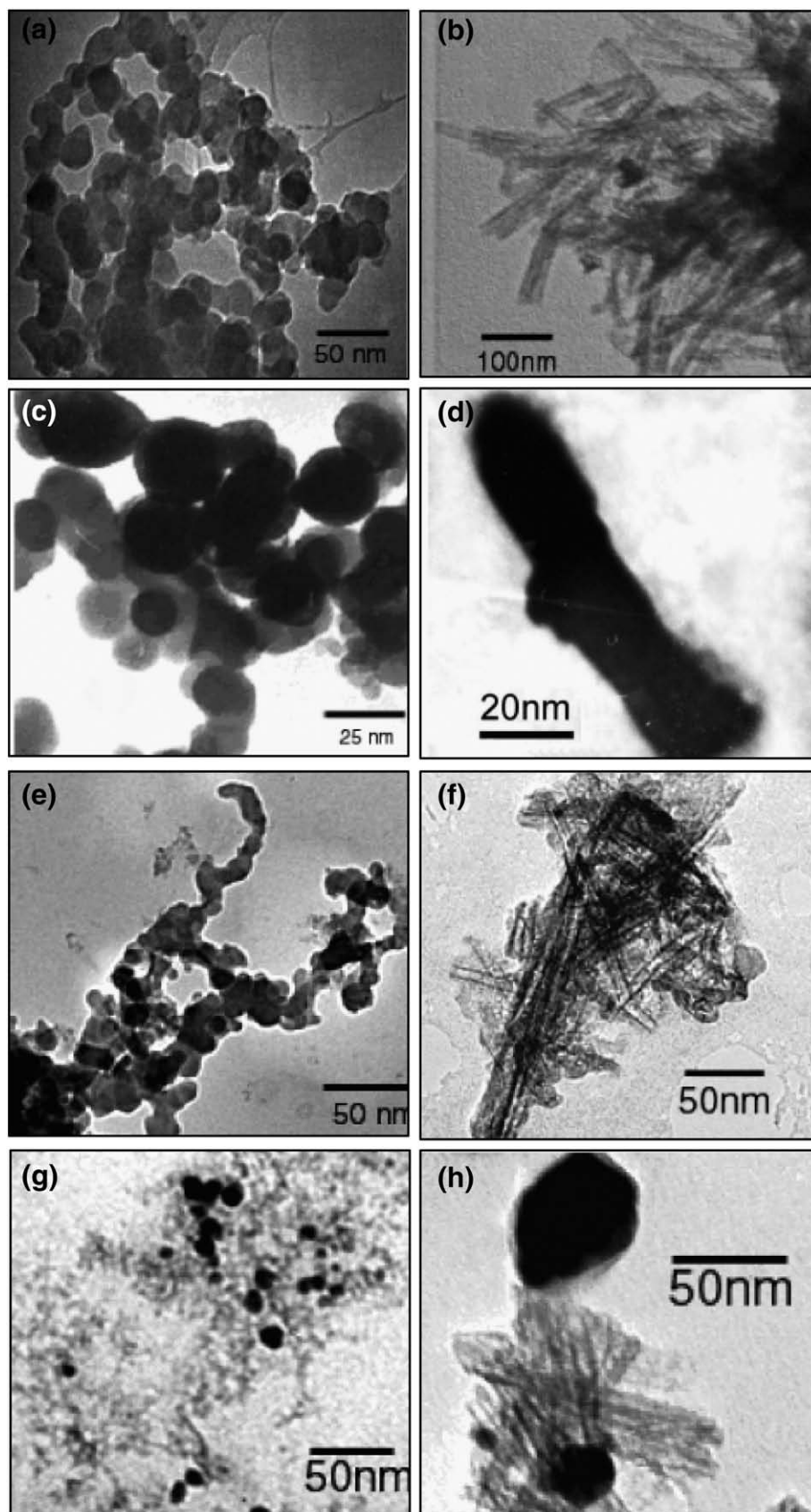


Fig. 7. The surface-plasmon absorbance spectrum of Ag NPs formed in the Tollens-PVA solution ( $\lambda_{\text{max}}=422$  nm).



**Fig. 8.** TEM images of (a) TiO<sub>2</sub> nanoparticles, (b) TiO<sub>2</sub> nanotubes, (c) Ag-TiO<sub>2</sub> nanoparticles, (d) Ag-TiO<sub>2</sub> nanotubes, (e) PVA-capped TiO<sub>2</sub> nanoparticles, (f) PVA-capped TiO<sub>2</sub> nanotubes, (g) Ag on PVA-capped TiO<sub>2</sub> nanoparticles, and (h) Ag on PVA-capped TiO<sub>2</sub> nanotubes (reproduced from [182]) with permission from the American Chemical Society).



**Table 1**

Minimum inhibition concentrations and minimum bactericidal concentrations of Ag particles prepared via reduction of  $[\text{Ag}(\text{NH}_3)_2]^+$  by various reducing saccharides at an ammonia concentration of  $0.005 \text{ mol L}^{-1}$  (data were taken from [66] with permission from the American Chemical Society)

Bacteria	Minimum inhibition and bactericidal concentrations ( $\mu\text{g/mL}$ )*					
	Glucose (44 nm)	Galactose (50 nm)	Maltose (25 nm)	Lactose (35 nm)	Cont <sup>a</sup>	Cont <sup>b</sup>
<i>Enterococcus faecalis</i> CCM 4224	–	–	13.5	54.0	6.75	–
<i>Staphylococcus aureus</i> CCM 3953	6.75	54.0	6.75	6.75	6.75	–
<i>Escherichia coli</i> CCM 3954	27.0	–	3.38	27.0	1.69	–
<i>Pseudomonas aeruginosa</i> CCM 3955	27.0	–	6.75	13.5	0.84	–
<i>Pseudomonas aeruginosa</i>	13.5	27.0	3.38	13.5	0.84	–
<i>Staphylococcus epidermidis</i> <sup>1</sup>	13.5	6.75	1.69	6.75	0.84	–
<i>Staphylococcus epidermidis</i> <sup>2</sup>	6.75	54.0	1.69	6.75	1.69	–
<i>Staphylococcus aureus</i> MRSA	27.0	54.0	6.75	27.0	6.75	–
<i>Enterococcus faecium</i> (VRE)	–	–	13.5	54.0	3.38	–
<i>Klebsiella pneumoniae</i> (ESBL-positive)	27.0	–	6.75	54.0	3.38	–

<sup>1</sup> (Methicillin-susceptible); <sup>2</sup> (methicillin-resistant); “–” growth inhibition of bacteria unsubstantiated.

\* MIC and MBC of silver sols had same values.

<sup>a</sup> Control sample containing all initial reaction components without reducing saccharides.

<sup>b</sup> Control sample containing all initial reaction components without silver nitrate.

Enhanced antibacterial activities have been reported in Ag NPs modified by surfactants, as SDS and Tween 80, and polymers, as PVP 360 [67]. The results are presented in Fig. 9. The antibacterial activity was significantly enhanced for most of the species when Ag NPs were modified with SDS (Fig. 9). However, the antibacterial effect of Tween 80 modified Ag NPs was not significant (Fig. 9). SDS provides more stability to Ag NPs than Tween 80; resulting in a higher antibacterial activity. Additionally, SDS is an ionic surfactant and may have the ability to penetrate or disrupt the cell wall, particularly of gram-positive strains [67,191]. Comparatively, Tween 80 is a non-ionic surfactant and may not be making contact with the cell wall [67]. The antibacterial activities of PVP modified Ag NPs were significant because the polymer is most effective in stabilizing particles against aggregation [67].

In another work, the effect of Ag NPs on bacterial growth of *E. coli*, *Vibria cholera*, *P. aeruginosa*, and *Syphilis typhus* has been studied using a high angle annular dark field (HAADF) scanning transmission electron microscopy (STEM) technique Fig. 10 [42,190]. Fig. 10 (b) and (c) demonstrate that this technique can identify presence of Ag NPs as small as  $\sim 1 \text{ nm}$ . No significant bacterial growth was observed at Ag NPs concentrations above  $75 \mu\text{g/mL}$ . Some noticeable damage to the cell membrane by Ag NPs could be seen (Figs. 10 (b) and 9 (e)). The damage to cell may be caused by interaction of Ag NPs with phosphorous- and sulfur-containing compounds such as DNA. Silver tends to have a high affinity for such compounds [192,193].  $\text{Ag}^+$  ions strongly interact with the available  $-\text{SH}$  groups of the biomolecule to inactivate the bacteria [194,195]. Furthermore, the antibacterial activity of  $\text{Ag}^+$  ion under anaerobic conditions was found less potent than in oxygen rich environment [195]. Such interactions in the cell membrane would prevent DNA replications [195,196], which would lead to bacterial death [195,197,198].

Involvement of interaction of Ag NPs with bacteria has also been shown in a study of amine-terminated hyperbranched poly(amidoamine) (HPAMAM- $\text{NH}_2$ )/Ag nanocomposites [199]. The nanocomposites had an average particle size of 15–4 nm and the antibacterial activity was tested against *S. typhus*, *E. coli*, *B. subtilis*, and *Klebsiella mobilis* [199]. The bacterial activity was inhibited up to 95% by low concentrations of the HPAMAM- $\text{NH}_2$ /Ag nanocomposite,  $2.7 \mu\text{g/mL}$ , and this was comparable to inhibition observed in Ag-doped  $\text{TiO}_2$ , Ag

NPs prepared with surfactant templates, and Ag NPs in a carbon matrix [195,200,201]. The strong interaction between negatively charged bacterial wall and HPAMAM- $\text{NH}_2$  macromolecules [202–204] can possibly decrease the distance between the Ag NPs and bacteria. This process could facilitate the release of active Ag into the bacteria resulting in a synergistic antibacterial effect of the HPAMAM- $\text{NH}_2$ /Ag nanocomposites [199].

In proteomic and biochemical studies, nanomolar concentrations of Ag NPs have killed *E. coli* cells within minutes possibly due to immediate dissipation of the proton motive force [205]. This action is similar to that found for antimicrobial activities of  $\text{Ag}^+$  ions [206]. For example, low concentrations of  $\text{Ag}^+$  ion result in massive proton leakage through the *Vibrio cholerae* membrane [206]. This proton leak might be happening from either any  $\text{Ag}^+$ -modified membrane protein or any  $\text{Ag}^+$ -modified phospholipids bilayer. The phenomenon causes deenergization of the membrane and consequently cell death [206]. Importantly, the determined effective concentration of Ag NPs was at nanomolar levels while  $\text{Ag}^+$  ions were effective at micromolar levels [205]. Ag NPs thus seem to be more efficient than  $\text{Ag}^+$  ions in performing antimicrobial activities. Picomolar levels of Ag NPs, on the other hand, have been used as nanoprobe in membrane penetration studies and did not create significant toxicity to the cells [207]. Moreover, the role of  $\text{Ag}^+$  ion in the antibacterial activity of Ag NPs was recently studied by partially oxidizing Ag NPs [208]. The oxygen can easily oxidize nano-Ag [78,209] to yield partially oxidized nano-Ag with chemisorbed  $\text{Ag}^+$  ions [208]. The antibacterial activities of Ag NPs against *E. coli* depended on the chemisorbed  $\text{Ag}^+$  ions (surface oxidation) and particle size.

The effect of shape on the antibacterial activity of Ag NPs has only recently been reported [210]. The Ag NPs of different shapes (triangular, spherical, and rod) were tested against *E. coli* [210]. The surfaces of untreated and treated bacterial cells were investigated by energy-filtering transmission electron microscopy (EFTEM). The {111} facets have high-atom-density, which is favorable for the reactivity of

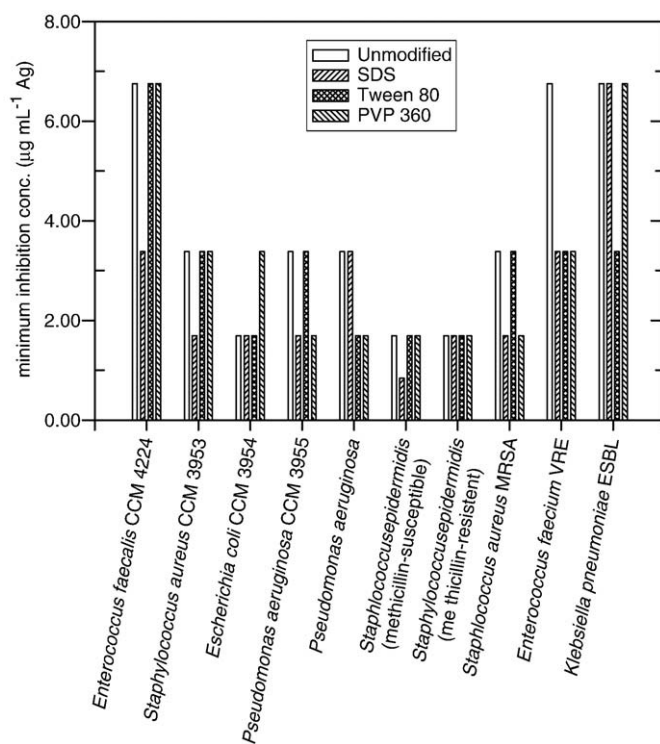


**Fig. 9.** A plot of minimum inhibition concentration (MIC) of the Ag NPs prepared by the modified Tollens process with D-maltose and consequently modified by addition of SDS, Tween 80, and PVP 360 in concentration of 1% (w/w). (Data were taken from [67] with permission from the American Chemical Society).

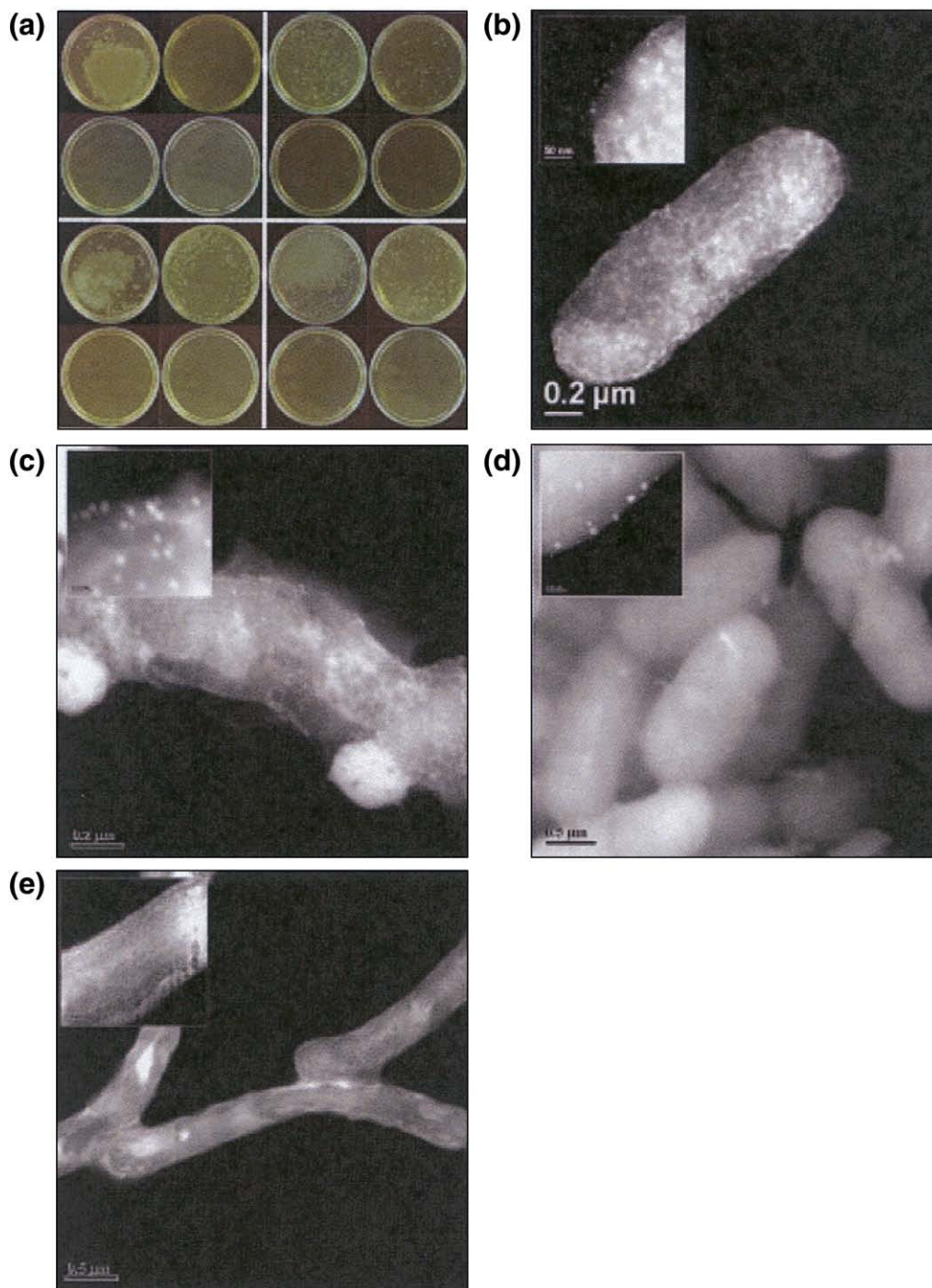


**Fig. 10.** (a) bacteria grown on agar plates at different concentrations of Ag NPs. Upper left, *E. coli*; upper right, *S. typhus*; bottom left, *P. aeruginosa*, and bottom right, *V. cholerae*.  $0 \mu\text{g mL}^{-1}$  (upper left),  $25 \mu\text{g mL}^{-1}$  (upper right),  $50 \mu\text{g mL}^{-1}$  (bottom left) and  $75 \mu\text{g mL}^{-1}$  (bottom right). HAADF STEM images that show the interaction of the bacteria with the Ag NPs: (b) *E. coli*, (c) *S. typhus*, (d) *P. aeruginosa*, and (e) *V. cholerae*. The inset correspond to higher magnification images. (reproduced from [190] with permission from the Institute of Physics).

Ag [211]. A triangular nanoplate has a high percentage of {111} facets whereas spherical and rod-shaped Ag NPs predominantly have {100} facets along with a small percentage of {111} facets [211].

### 5.2. The battle against infection: Ag NPs and their incorporation into the medical field

In hospitals, infection is the most common complication and cause of death in patients. Therefore, antibacterial effects of Ag have been incorporated into various medical applications. Plastic catheters coated with Ag NPs prevent biofilm formation from *E. coli*, *Enterococcus*,

*Staphylococcus aureus*, *Candida albicans*, *Staphylococci*, and *Pseudomonas aeruginosa* and also show significant *in vitro* antimicrobial activity [212]. Silver aerosol NPs were efficient as antimicrobial agents against *B. subtilis* [213]. Polymethylmetacrylate (PMMA) bone cement loaded with Ag NPs has shown clinical use [183]. Supplementation of Ag NPs with antibiotics as penicillin G, amoxicillin, erythromycin, clindamycin, and vancomycin against *E. coli* and *S. aureus* has been examined [214]. The presence of Ag NPs increased the antibacterial activities of antibiotics for both strains [214]. Additionally, Ag NPs-embedded paints demonstrated killing of both Gram-positive human pathogens and Gram-negative bacteria [215].

### 5.2.1. Ag NPs and HIV

Recently, a study revealed the potential cytoprotective activity of Ag NPs toward HIV-1 infected cells [216]. The activity of Ag NPs towards HIV-1 infected Hut/CCR5 cells was investigated using terminal uridyl-nucleotide end labeling (TUNEL) assay after a three day treatment [216]. The percentage of apoptotic cells were determined as 49%, 35%, and 19% for vehicle control, 5  $\mu\text{M}$  Ag, and 50  $\mu\text{M}$  Ag, respectively. Ag NPs might inhibit the replication in Hut/CCR5 cells causing HIV-associated apoptosis [216]. Size dependent interaction of Ag NPs with HIV-1 virus has also been demonstrated [217]. Ag NPs preferentially binds to gp120 glycoprotein knobs of HIV-1 virus. In the vitro study, it was further shown that this interaction caused the virus not to bind with the host cell [217].

### 5.3. Antibacterial water filter

According to the World Health Organization (WHO), point-of-use treatment has the potential to improve the microbial quality of water

and reduce the risk of water related diseases such as diarrhea and dehydration [218,219]. Ag NPs on polyurethane foam were stable and were not washed away by water flow, possibly due to its interaction with the nitrogen atom of polyurethane [220]. The foam was tested with an *E. coli* load of  $10^5$  CFU  $\text{mL}^{-1}$  at a flow rate of  $0.5 \text{ L min}^{-1}$ . Within seconds, the output count of *E. coli* in the effluent was below the detection limit [220]. Also, few studies have been conducted on Ag containing carbon filters for their ability to reduce bactericidal activity [221–223]. Bacteria and fungi were tested and strong lethal activity against *E. coli*, *Saccharomyces cerevisiae*, and *Pichia pastoris* was observed within a few seconds [221]. The use of reactive oxygen species (ROS), a scavenger, and  $\text{Ag}^+$  ion, a neutralizing agent, suggested a role of ROS in the strong bactericidal activity of carbon filter supporting silver [222].

Colloidal-Ag-impregnated ceramic filters were recently tested for household water treatment in the laboratory [224]. The filters removed  $\sim 97.8\%$ – $100\%$  of the *E. coli*. Initially, Ag concentrations in the effluent filter water were greater than  $0.1 \text{ mg L}^{-1}$ , but decreased to  $<0.1 \text{ mg L}^{-1}$  after  $\sim 200$  min. Overall, the findings suggest the use of the ceramic filters as an effective and sustainable point-of-use water treatment technology.

### 5.4. Antimicrobial air filter

Bioaerosols are airborne particles of biological origins, which are capable of causing acute and chronic diseases [225]. Generally, bioaerosols accumulate on ventilating, heating, and air-conditioning systems with a tendency to multiply under humid conditions [226]. Activated carbon fiber (ACF) filters are widely used for removal of hazardous gaseous pollutants from the air. However, ACF filters themselves become a source of bioaerosols because bacteria preferentially adhere to carbon solid materials [227,228].

The antimicrobial effect of Ag particles coated onto an ACF filter was recently tested [229,230]. Ag-deposited ACF filters were effective for the removal of bioaerosols. The results of the test filters on *E. coli* and *B. subtilis* are shown in Fig. 11. The ACF/Ag-10, ACF/Ag-20, and ACF/Ag-30 represent samples prepared with metal solution at deposition times of 10, 20, and 30 min, respectively without using electric current [230]. The colony ratios ( $C/C_0$ ) of both *E. coli* and *B. subtilis* increased with time suggesting multiplication of bacteria on the pristine ACF filters [230]. However, the colony ratios decreased for Ag-containing ACF filters; the decrease was sharper for *B. subtilis* than for *E. coli* species (Fig. 11). Due to low resistivity of *B. subtilis*, inhibition took place in about 10 min [230]. Comparatively, *E. coli* was fully inhibited after 60 min using a Ag-containing ACF filters [230].

## 6. Implications

### 6.1. Human Health

Nanoparticles may have different effects on human health relative to bulk material from which they are produced [15]. Increase in biological activity of nanoparticles can be beneficial, detrimental or both. Many nanoparticles are small enough to have an access to skin, lungs, and brain [15,231,232]. Currently, no sufficient information is available on the adverse effects of nanoparticles on human health [233], but studies are forthcoming to address this subject [234–239]. Exposure of metal-containing nanoparticles to human lung epithelial cells generated reactive oxygen species, which can lead to oxidative stress and cellular damage [240,241]. Nanoparticles and reactive oxygen production have an established link *in vivo* [242,243]. A study on toxic effects of Ag NPs was done on zebrafish as a model due to its fast development and transparent body structure [244]. The results showed a deposition of particles on organs and severe developmental effects [244]. Similar results of Ag NPs toxicity were observed during zebrafish embryogenesis [245].

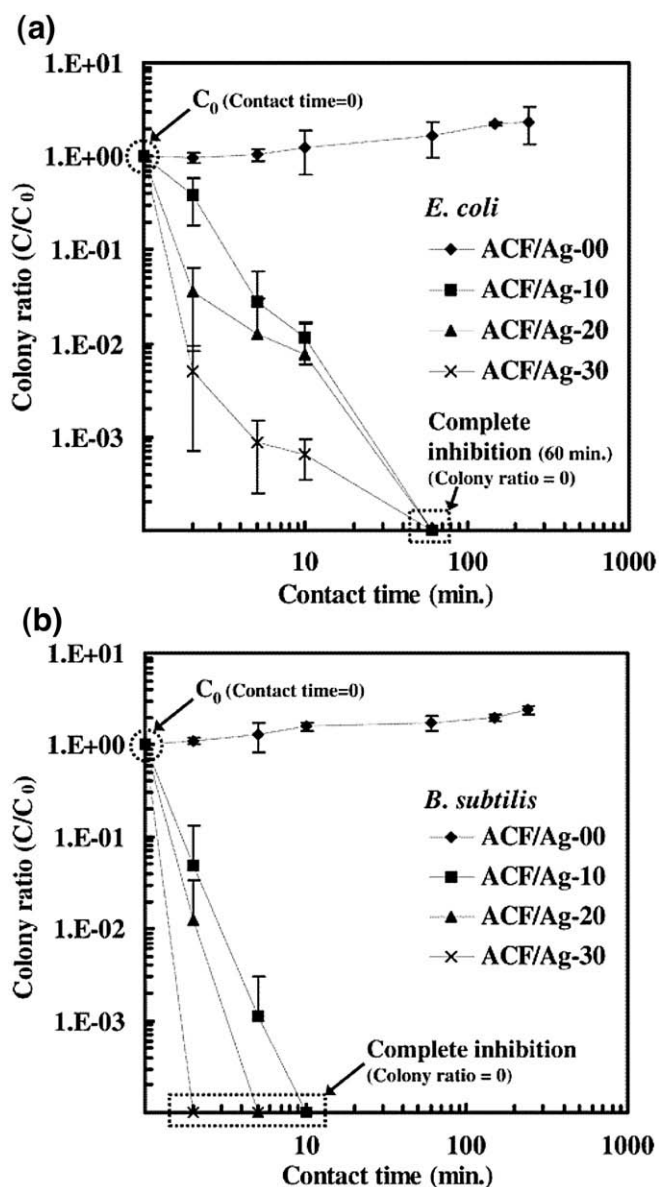


Fig. 11. Antimicrobial effects of the test filters on *E. coli* (a) and *B. subtilis* (b).  $C_0$  and  $C$  are colony count at contact time 0 and  $t$  minutes, respectively. (reproduced from [230] with permission from the American Chemical Society).

## 6.2. Environmental

The increasing use of consumer nanotechnological products may result in an increased release of NPs into the aquatic environment [246–248]. Though regulation exists for protecting aquatic species from soluble forms of toxic metals, it is critical to understand the toxicity of metallic nanoparticles [249–252]. The studies on the effect of Ag NPs on biological species are forthcoming [253–256]. As discussed previously, proteomic analysis (2-DE and MS identification) was conducted to observe the mode of the antibacterial effect of Ag NPs against *E. coli* [253]. An accumulation of envelope protein precursors due to Ag NPs occurred, which suggests the dissipation of proton motive force [253]. Furthermore, the proteomic data indicate that Ag NPs destabilized the outer membrane, which resulted in a collapse of the plasma membrane potential and depletion of intracellular ATP levels [253].

Single-NP probes (individual Ag NPs) were developed to study real time transport, biocompatibility, and toxicity of Ag NPs in the early development of zebrafish embryos [254]. It was found that single Ag NPs with an average diameter of  $11.6 \pm 3.5$  nm were transported in and out of embryos through chorion pore canals. The Brownian diffusion,  $3 \times 10^{-9} \text{ cm}^2 \text{ s}^{-1}$ , inside the chorionic space was determined [254]. The biocompatibility and toxicity of Ag NPs were exhibited by observing single Ag NPs inside embryos at each development stage. The types of abnormalities in zebrafish were strongly dependent on the dose of Ag NPs [254]. Fish can bioconcentrate trace contaminants in the aquatic environment and the potential release of nanomaterials may also affect human health through the consumption of fish.

Furthermore, Ag NPs are of great concern to wastewater treatment utilities and to biological systems [255]. The inhibitory effects of Ag NPs on microbial growth were evaluated at a treatment facility using an extant respirometry technique [255]. The nitrifying bacteria were susceptible to inhibition by Ag NPs, which could have detrimental effects on the microorganisms in wastewater treatment. The environmental risk of Ag NPs was recently investigated by determining released Ag from commercial clothing (socks) [256]. The sock material and wash water contained Ag NPs of 10–500 nm diameter. The fate of Ag in wastewater treatment plants (WWTPs), which could treat a high concentration of influent Ag, was also examined [256]. The model suggested that WWTPs are capable of removing Ag at concentrations much more than expected from the Ag NPs-containing consumer products. However, Ag concentrations in the biosolids may exceed the concentration (5 mg/L), established by the USEPA. This may restrict the fertilizer application of biosolids to the agricultural lands.

## 7. Concluding remarks

Several synthetic methods for Ag NPs using inexpensive and nontoxic compounds under water environments were summarized and experimental approaches under different conditions were given to control the morphology of the Ag particles. Rapid and green synthetic methods using extracts of bio-organisms have shown a great potential in Ag NP synthesis. However, understanding the mechanism by which biomolecules of these organisms are involved in synthesis is lacking. A progress in this area will give new green paths in the development of controlled shape and size Ag NPs. Custom designed biomolecules can then be made to synthesize Ag NPs, which will in turn fill the gap between biological synthesis and biometric synthesis. Moreover, the syntheses of nanostructures of Ag in high yield and in a wide range of shapes are challenging tasks. This requires the understanding of the nuclei formation and the influence of reaction species on nuclei morphology [24]. The theoretical calculations in conjunction with high-resolution mass spectrometry will help to achieve this objective [257].

Silver incorporated into polymer and  $\text{TiO}_2$  surfaces have favorable electronic, photo and catalytic properties. Different synthetic

approaches for the surface modification were provided resulting in different particle morphologies. Surfactants and polymers modified Ag NPs have advantages in antibacterial activities; however their antibacterial actions are not fully understood. The techniques to measure transport of Ag NPs *in vivo* in real time scales are needed to make headways in observing particle interactions. Some progress was made in a recent study [254] and more such studies should occur in the future. This will also determine the effect of Ag NPs on important aquatic species and reveal their environmental consequences.

The increasing use of Ag NPs in consumer products will increase their release to the environment and any advancement in nanotechnology would thus require assessment of environmental risks associated with these particles [15,258]. The ecotoxic studies on the exposure of Ag NPs need an analytical technique that can distinguish nano-Ag metal from the dissolved  $\text{Ag}^+$  species under environmental conditions. Such techniques are becoming more available, but their applications at relatively low concentrations are still limited [259,260].

## Acknowledgment

We wish to thank three anonymous reviewers for their useful comments that greatly improved this paper.

## References

- [1] Dahl JA, Maddux BLS, Hutchison JE. *Chem Rev* 2007;107:2228.
- [2] Hutchison JE. *ACS Nano* 2008;2:395.
- [3] Anstas PT, Warner JC. *Green Chemistry: Theory and Practice*. New York: Oxford University Press, Inc.; 1998.
- [4] DeSimone JM. *Science* 2002;297:799.
- [5] Cross RA, Kalra B. *Science* 2002;297:803.
- [6] Poliakoff M, Anastas T. *Nature* 2001;413:257.
- [7] Raveendran P, Fu J, Wallen SL. *J Am Chem Soc* 2003;125:13940.
- [8] Li L, Hu J, Alivisatos AP. *Nano Lett* 2001;1:349.
- [9] Hussain I, Brust M, Papworth AJ, Cooper AI. *Langmuir* 2003;19:4831.
- [10] Burleson DJ, Driessen MD, Penn RL. *J Environ Sci Health A* 2005;39:2707.
- [11] Cheng M-D. *J Environ Sci Health A* 2005;39:2691–705.
- [12] Obare SO, Meyer GJ. *J Environ Sci Health A* 2005;39:2549.
- [13] Yuan G. *J Environ Sci Health A* 2005;39:2545.
- [14] Masciangioli T, Zhang W-X. *Environ Sci Technol* 2003;37:102A–8A.
- [15] Albrecht MA, Evans CW, Raston CL. *Green Chem* 2006;8:417.
- [16] Smith AM, Duan H, Rhyner MN, Ruan G, Nie SA. *Phys Chem Chem Phys* 2006;8:3895.
- [17] Kearns GJ, Foster EW, Hutchison JE. *Anal Chem* 2006;78:298.
- [18] Burda C, Chen X, Narayanan R, El-Sayed MA. *Chem Rev* 2005;105:1025.
- [19] Tessier PM, Velev OD, Kalambur AT, Rabolt JF, Lenhoff AM, Kaler EW. *J Am Chem Soc* 2000;122:9554.
- [20] Mulvaney P. *Langmuir* 1996;12:788.
- [21] Knoll B, Keilmann F. *Nature* 1999;399:134.
- [22] Sengupta S, Eavarone D, Capila I, Zhao GL, Watson N, Kiziltepe T, et al. *Nature* 2005;436:568.
- [23] Brigger I, Dubernet C, Couvreur P. *Adv Drug Deliv Rev* 2004;54:6310.
- [24] Alivisatos P. *Nat Biotechnol* 2004;22:47.
- [25] Gao XH, Cui YY, Levenson RM, Chung LWK, Nie SM. *Nat Biotechnol* 2004;22:969.
- [26] Singh M, Singh S, Prasad S, Gambhir IS. *Dig J Nanomater Biostruct* 2008;3:115.
- [27] Chen W, Cai W, Zhang L, Wang G, Zhang L. *J Colloid Interface Sci* 2001;238:291.
- [28] Frattini A, Pellegri N, Nicastro D, de Sanctis O. *Mater Chem Phys* 2005;94:148.
- [29] Wiley B, Sun Y, Xia Y. *Acc Chem Res* 2007;40:1067.
- [30] Nagy A, Mestl G. *Appl Catal A* 1999;188:337.
- [31] Frattini A, Pellegri N, Nicastro D, de Sanctis O. *Mater Chem Phys* 2005;94:148.
- [32] Cao YW, Jin RC, Mirkin CA. *Science* 2002;297:1536.
- [33] Rosi NL, Mirkin CA. *Chem Rev* 2005;105:1547.
- [34] Belloni J. *Radiat Phys Chem* 2003;67:291.
- [35] Tao A, Sinsersuksaku P, Yang P. *Angew Chem Int Ed* 2006;45:4597.
- [36] Wiley B, Sun Y, Mayers B, Xi Y. *Chem-Eur J* 2005;11:454.
- [37] Lee PC, Meisel D. *J Phys Chem* 1982;86:3391.
- [38] Shirlcliffe N, Nickel U, Schneider S. *J Colloid Interface Sci* 1999;211:122.
- [39] Nickel U, Castell AZ, Poppl K, Schneider S. *Langmuir* 2000;16:9087.
- [40] Chou K-S, Ren C-Y. *Mater Chem Phys* 2000;64:241.
- [41] Evanoff Jr D, Chumanov GJ. *J Phys Chem B* 2004;108:13948.
- [42] Sondi I, Goia DV, Matijević E. *J Colloid Interface Sci* 2003;260:75.
- [43] Merga G, Wilson R, Lynn G, Milosavljević BH, Meisel D. *J Phys Chem C* 2007;111:12220.
- [44] Creighton JA, Blatchford CG, Albrecht MJ. *J Chem Soc Faraday Trans* 1979;75:7902.
- [45] Ahmadi TS, Wang ZL, Green TC, Henglein A, El-Sayed M. *Science* 1996;272:1924.
- [46] Kapoor S, Lawless D, Kennepohl P, Meisel D, Serpone N. *Langmuir* 1994;10:3018.



- [179] Li H, Duan X, Liu G, Liu X. *J Mater Sci* 2008;43(5):1669.
- [180] Miao L, Ina Y, Tanemura JT, Tanemura M, Kaneko K, Toh S, et al. *Surf Sci* 2007;601(13):2792.
- [181] Zeng H, Zhao C, Qiu J, Yang Y, Chen G. *J Cryst Growth* 2007;300(2):519.
- [182] Guin D, Manorama SV, Latha JNL, Singh S. *J Phys Chem C* 2007;111(36):13393–7.
- [183] Alt V, Bechert T, Steinrück P, Wagener M, Seidel P, Dingeldein E, et al. *Biomaterials* 2004;25:4383.
- [184] Russell AD, Hugo WB. *Prog Med Chem* 1994;31:351.
- [185] Lee HY, Park HK, Lee YM, Kim K, Park SB. *Chem Commun* 2007:2959.
- [186] Jeong S, Yeo S, Yi S. *J Mater Sci* 2005;40:5407.
- [187] Chou W-L, Yu D-G, Yang M-C. *Polym Adv Technol* 2005;16(8):600.
- [188] Jin M, Zhang X, Nishimoto S, Liu Z, Tryk DA, Emeline AV, et al. *J Phys Chem C* 2007;111:658.
- [189] Chen Q, Yue L, Xie F, Zhou M, Fu Y, Zhang Y, et al. *J Phys Chem C* 2008;112:10004.
- [190] Morones JR, Elechiguerra JL, Camacho A, Holt K, Kouri J, Ramirez JT, et al. *Nanotechnology* 2005;16:2346.
- [191] Carpenter PL. *Microbiology*. Philadelphia: W.B. Saunders Company; 1972. p. 245.
- [192] Hatchert DW, Henry SJ. *J Phys Chem* 1996;100:9854.
- [193] Basu S, Jana S, Pande S, Pal T. *J Colloid Int Sci* 2008;321:288.
- [194] Gupta A, Maynes M, Silver S. *Appl Environ Microbiol* 1998;64:5042.
- [195] Matsumura Y, Kuniaki Y, Kunisaki S-I, Tsuchido T. *Appl Environ Microbiol* 2002;69:4278.
- [196] Nover L, Scharf KD, Neumann D. *Mol Cell Biol* 1983;3:1648.
- [197] Melaiye A, Sun Z, Hindi K, Milsted A, Ely D, Reneker DH, et al. *J Amer Chem Soc* 2005;127:2285.
- [198] Feng QL, Wu J, Chen GQ, Cui FZ, Kim TN, Kim JO. *J Biomed Mater Res* 2000;52:662.
- [199] Zhang Y, Peng H, Huang W, Zhou Y, Zhang X, Yan D. *J Phys Chem C* 2008;112:2330.
- [200] Sondi I, Salopek-Sondi B. *J Colloid Int Sci* 2004;275:177.
- [201] Thiel J, Pakstis L, Buzby S, Raffi MNC, Pochan DJ, Shah SI. *Small* 2007;3:799.
- [202] Ye WJ, Leung MF, Xin J, Kwong TL, Lee DKL, Li P. *Polymer* 2005;46:10538.
- [203] Sambhy V, MacBride MM, Peterson BR, Sen A. *J Am Chem Soc* 2006;128:9798.
- [204] Lenoir S, Pagnoulle C, Detrembleur C, Galleni M, Jerome R. *J Polym Sci Part A Polym Chem* 2006;44:1214.
- [205] Lok C-N, Ho C-M, Chen R, He Q-Y, Yu W-Y, Sun H, et al. *J Proteome Res* 2006;5:916.
- [206] Dibrov P, Dzioba J, Gosini KK, Hase CC. *Antimicrob Agents Chemother* 2002;46:2668.
- [207] Xu X-HN, Brownlow WJ, Kyriacou SV, Wan Q, Viola JJ. *Biochemistry* 2004;43:10400.
- [208] Lok C-N, Ho C-M, Chen R, He Q-Y, Yu W-Y, Sun H, et al. *J Biol Inorg Chem* 2005;12:527.
- [209] Henglein A. *Chem Mater* 1998;10:444.
- [210] Pal S, Tak YK, Song JM. *Appl Environ Microbiol* 2007;73:1712.
- [211] Wiley BY, Sun BM, Xia Y. *Chem Eur J* 2005;11:454.
- [212] Roe D, Karandikar B, Bonn-Savage N, Gibbins B, Roulet J-B. *J Antimicrob Chemother* 2008;61(4):869.
- [213] Yoon K-Y, Byeon JH, Park J-H, Ji JH, Bae GN, Hwang J. *Environ Eng Sci* 2008;25(2):289.
- [214] Shahverdi AR, Fakhimi A, Shahverdi HR, Minaian. *Nanomed Nanotech Biol Med* 2007;3:168.
- [215] Kumar A, Vemula PK, Ajayan M, John G. *Nat Mater* 2008;7(3):23.
- [216] Sun RWY, Chen R, Chung NP-Y, Ho C-M, Lin C-L, Che C-M. *Chem Commun* 2005;40:5059.
- [217] Elechiguerra JL, Burt JL, Morones JR, Bragado AC, Gao X, Lara HH, et al. *J Nanotechnol* 2005;3:6 <http://www.jnanobiotechnology.com/content/3/1/6>.
- [218] Clasen TF, Brown J, Collins S, Suntura O, Cairncross S. *Am J Trop Med Hyg* 2004;70(6):651.
- [219] Sobsey MD. Managing water in the home: Accelerated health gains from improved water supply. World Health Organization; 2002. [http://who.int/water\\_sanitation\\_health/dwq/wsh0207/en/](http://who.int/water_sanitation_health/dwq/wsh0207/en/).
- [220] Jain P, Pradeep T. *Biotechnol Bioeng* 2005;90(1):59.
- [221] Lepape H, Solano-Serena F, Contini P, Devillers C, Maftah A, Leprat P. *Carbon* 2002;40(15):2947.
- [222] Lepape H, Solano-Serena F, Contini P, Devillers C, Maftah A, Leprat P. *J Inorg Biochem* 2004;98:1054.
- [223] Hector O-I, Norberto C, Victor S, Maximiliano B-S, Refugio T-V, Wencel DLC, et al. *J Colloid Interface Sci* 2007;314:562.
- [224] Oyanedel-Craver VA, Smith JA. *Environ Sci Technol* 2008;42:927.
- [225] Main CE. *Environ Int* 2003;29:347.
- [226] Maus R, Goppelsroder A, Umhauer H. *Atmos Environ* 2001;35:105.
- [227] Park SJ, Jang YS. *J Colloid Interface Sci* 2003;261:238.
- [228] Byeon JH, Yoon KY, Park JH, Hwang J. *Carbon* 2007;45:2313.
- [229] Foss Manufacturing Co Inc. *Filtr Sep* 2004;41:26.
- [230] Yoon KI, Byeon JH, Park CW, Hwang J. *Environ Sci Technol* 2008;42:1251.
- [231] Koziara JM, Lockman PR, Allen DD, Mumper RJ. *Pharm Res* 2003;20:1772.
- [232] Oberdorster G, Sharp Z, Atudorei V, Elder A, Gelein R, Kreyling W, et al. *Inhal Toxicol* 2004;16:437.
- [233] Lubick N. *Environmental Science Technology On Line News*; February 20, 2008.
- [234] Oberdorster G, Oberdorster E, Oberdorster J. *Environ Health Perspect* 2005;113:823.
- [235] Kreyling WG, Semmler-Behnke M, Moller W. *J Nanopart Res* 2006;8:543.
- [236] Gwinn MR, Vallyathan V. *Environ Health Perspect* 2006;114:1818.
- [237] Linse S, Cabaleiro C, Xue W-F, Lynch I, Lindman S, Thulin E, et al. *Proc Natl Acad Sci U S A* 2007;104:8691.
- [238] Schmid K, Riediker M. *Environ Sci Technol* 2008;42:2253.
- [239] Conti JA, Killpack K, Gerritzen G, Huang L, Mircheva M, Delmas M, et al. *Environ Sci Technol* 2008;42:3155.
- [240] Limbach LK, Wick P, Manser P, Grass RN, Bruinink, Stark WJ. *Environ Sci Technol* 2007;41:4158.
- [241] Xi T, Kovochich M, Brant J, Hotze M, Semp J, Oberley T, et al. *Nano Lett* 2006;6:1794.
- [242] Park S, Lee YK, Jung M, Chung N, Ahn EK, Lim Y, et al. *Inhal Toxicol* 2007;19(Suppl1):59.
- [243] Carter JM, Corson N, Driscoll KE, Elder A, Finkelstein JN, Harkema JN, et al. *J Occup Environ Med* 2006;48:1265.
- [244] Asharani PV. *Nanotechnology* 2008;19:255102.
- [245] Yeo M-K, Kang M. *Bull Korean Chem Soc* 2008;29:1179.
- [246] Moore MN. *Environ Int* 2006;32:967.
- [247] Lovern SB, Klaper R. *Environ Toxicol Chem* 2006;25:1132.
- [248] Service RF. *Science* 2004;304:1732.
- [249] Griffitt RJ, Weil R, Hyndman KA, Denslow ND, Powers K, Taylor D, et al. *Environ Sci Technol* 2007;41(23):8178.
- [250] Schmid K, Riediker M. *Environ Sci Technol* 2008;42(7):2253.
- [251] Chang M-D. *J Environ Sci Health A* 2005;39:2691.
- [252] Burleson DJ, Driessen MD, Penn RL. *J Environ Sci Health A* 2005;39:2707.
- [253] Lok V-N, Ho C-M, Chen R, He Q-Y, Yu W-Y, Sun H, et al. *J Proteome Res* 2006;5(4):916.
- [254] Lee KJ, Nallathamby, Browning LM, Osgood CJ, Xu XHN. *ACS Nano* 2007;1(2):133.
- [255] Choi C, Deng KK, Kim N-J, Ross Jr L, Rao YS, Hu Z. *Water Res* 2008;42:3066.
- [256] Benn TM, Westerhoff P. *Environ Sci Technol* 2008;42(18):7025.
- [257] Xiong Y, Washio I, Chen J, Sadilek M, Xia Y. *Angew Chem Int Ed* 2007;46:4917.
- [258] Scheufeile DA, Corley EA, Dunwoody S, Shih T-J, Hillback E, Guston DH. *Nat Nanotechnol* 2007;2:732.
- [259] Limbach LK, Wick P, Manser P, Grass RN, Stark WJ. *Environ Sci Technol* 2007;41:4158.
- [260] Liu FK, Ki FH, Huang PW, Wu CH, Chu TC. *J Chromatogr A* 2005;1062(1):139.